

New Journal of Chemistry

ELECTRONIC SUPPLEMENTARY INFORMATION

Tri- and tetraarylanthracenes with novel λ , χ and ψ topologies as blue-emissive as well as fluorescent host materials in organic light-emitting diodes (OLEDs)

Samik Jhulki,^a Alankriti Bajpai,^a Honnappa Nagarajaiah,^a Tahsin J. Chow,^{b,*}
and Jarugu Narasimha Moorthy^{a,*}

^aDepartment of Chemistry, Indian Institute of Technology, Kanpur 208016, INDIA

^bInstitute of Chemistry, Academia Sinica, Taipei, Taiwan 115, Republic of China

Email: chowtj@gate.sinica.edu.tw; moorthy@iitk.ac.in

Table of Contents

1	General aspects	S2
2	TGA profiles of ANT1-3	S2
3	DSC profiles of ANT1-3	S3
4	CV profiles of ANT1-3	S3
5	Plots of external quantum efficiency vs current density, external quantum efficiency vs luminance, luminous efficiency vs current density, luminous efficiency vs luminance, power efficiency vs current density and power efficiency vs luminance for the nondoped devices of configuration A-C	S4-S6
6	Plots of external quantum efficiency vs current density, external quantum efficiency vs luminance, luminous efficiency vs current density, luminous efficiency vs luminance, power efficiency vs current density and power efficiency vs luminance for the doped devices of configurations E and F	S7
7	¹ H NMR spectrum of ANT1	S8
8	¹³ C NMR spectrum of ANT1	S9
9	¹ H NMR spectrum of ANT2	S10
10	¹³ C NMR spectrum of ANT2	S11
11	¹ H NMR spectrum of ANT3	S12
12	¹³ C NMR spectrum of ANT3	S13
13	X-ray crystal structure determinations	S14-S16

General aspects. ^1H NMR spectra were recorded on JEOL (400/500 MHz) spectrometers in CDCl_3 as a solvent. ^{13}C NMR spectra were recorded on JEOL-Lambda (100/125 MHz) spectrometers with complete proton decoupling. ESI and EI mass spectra analyses were carried out on Waters $^{\text{Q}}$ TOF and GCT premier mass spectrometers, respectively. Melting points were determined with a JSGW melting point apparatus. IR spectra were recorded on a Bruker Vector 22 FT-IR spectrophotometer. The TGA and DSC measurements were carried out using Mettler-Toledo and SDT Q600 instruments, respectively, at $10\text{ }^\circ\text{C}/\text{min}$ under a nitrogen gas atmosphere. UV-vis absorption spectra were recorded on a Shimadzu UV-1800 spectrophotometer. PL measurements in solution and solid state were carried out using FluoroMax-4; FM4-3000 spectrofluorimeter, Horiba Scientific. Cyclic voltammetry measurements were performed using CHI610E electrochemical work-station (CH instruments, Texas, USA). All solvents were distilled prior to use, and HPLC grade solvents used for UV-vis and PL measurements were procured from Merck. Column chromatography was conducted with a silica gel of $100\text{-}200\mu$ mesh.

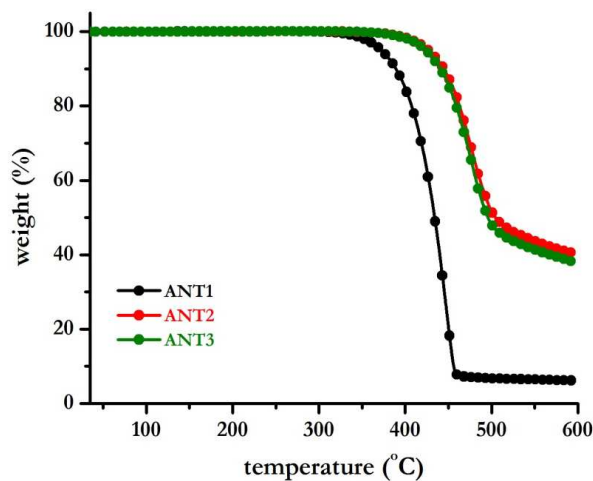


Fig. S1 TGA profiles of ANT1-3.

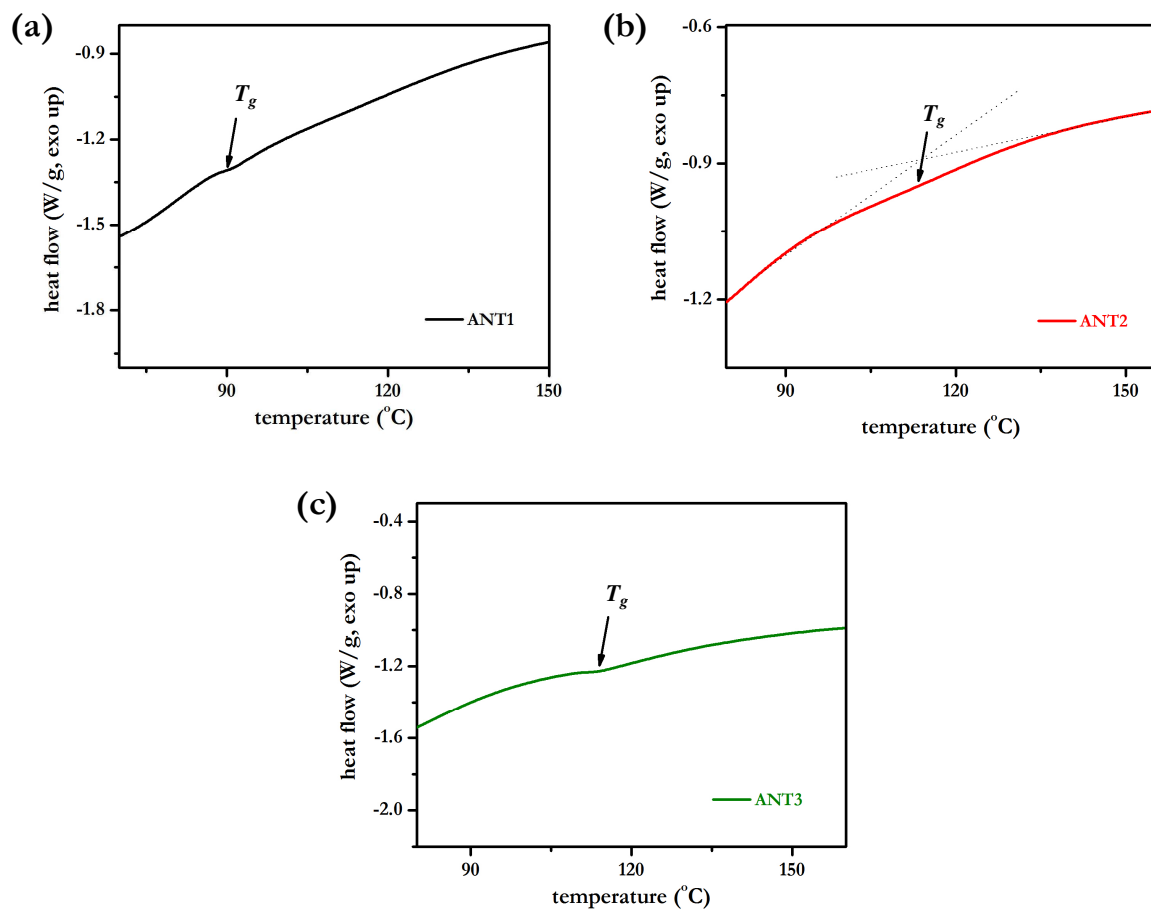


Fig. S2 DSC profiles of ANT1-3.

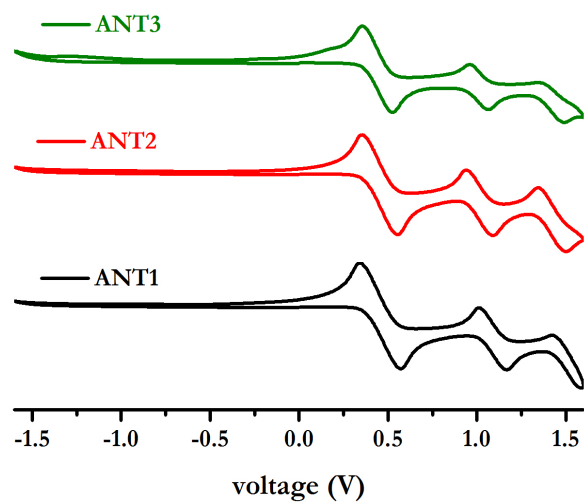


Fig. S3 CV profiles of ANT1-3.

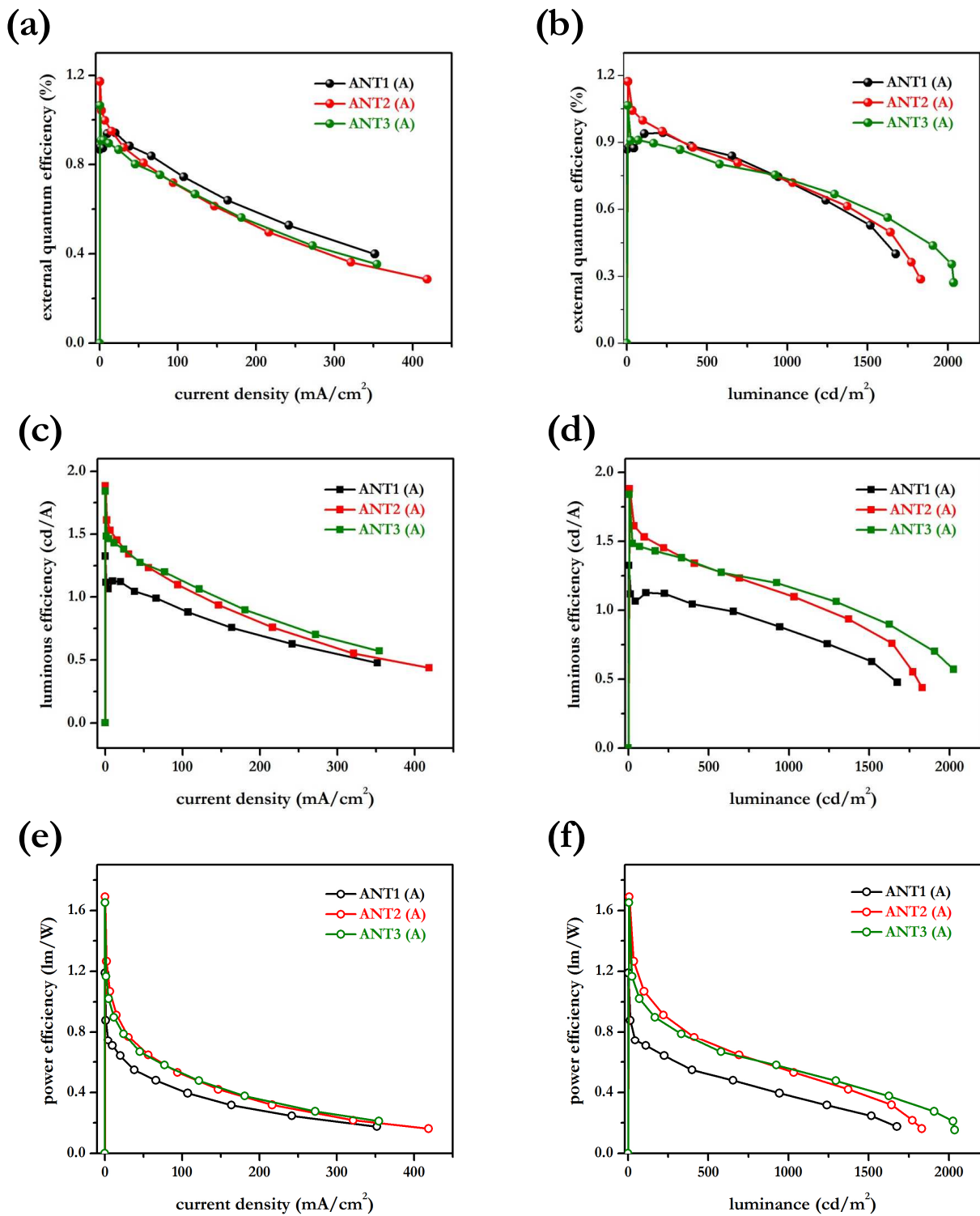


Fig. S4 Plots of external quantum efficiency vs current density (a), external quantum efficiency vs luminance (b), luminous efficiency vs current density (c), luminous efficiency vs luminance (d), power efficiency vs current density (e) and power efficiency vs luminance (f) for the devices of configuration A, refer to text.

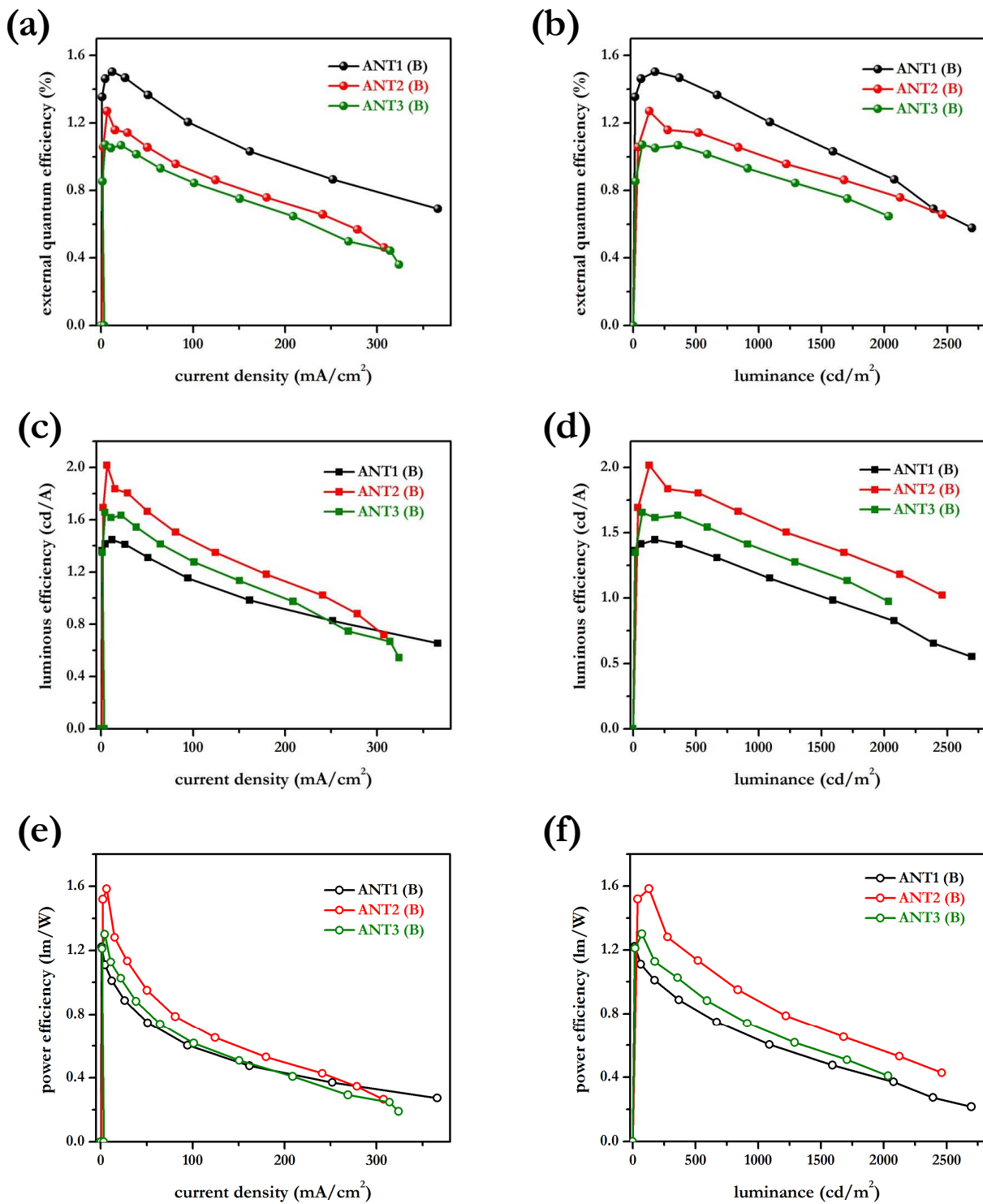


Fig. S5 Plots of external quantum efficiency vs current density (a), external quantum efficiency vs luminance (b), luminous efficiency vs current density (c), luminous efficiency vs luminance (d), power efficiency vs current density (e) and power efficiency vs luminance (f) for the devices of configuration B, refer to text.

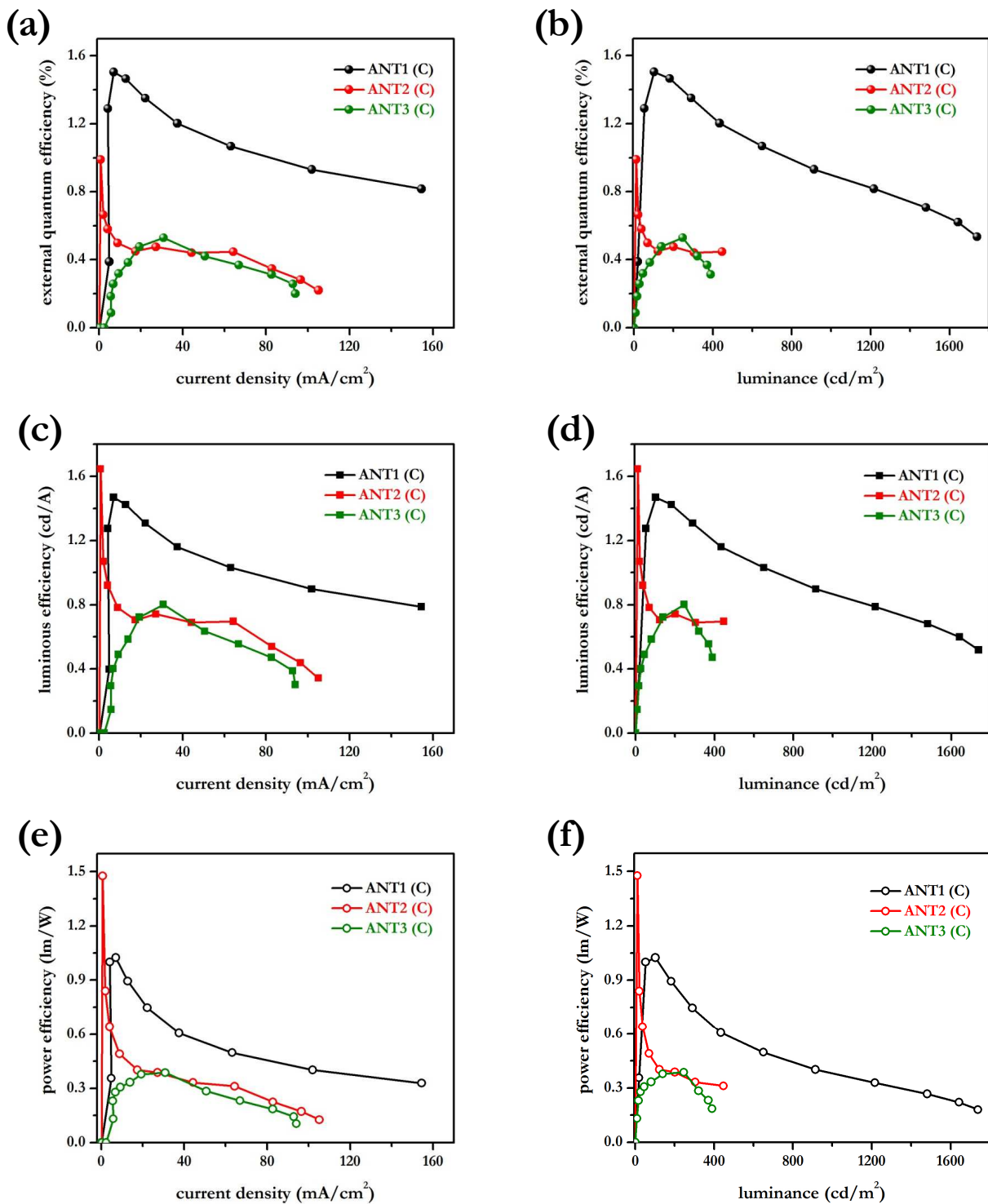


Fig. S6 Plots of external quantum efficiency vs current density (a), external quantum efficiency vs luminance (b), luminous efficiency vs current density (c), luminous efficiency vs luminance (d), power efficiency vs current density (e) and power efficiency vs luminance (f) for the devices of configuration C, refer to text.

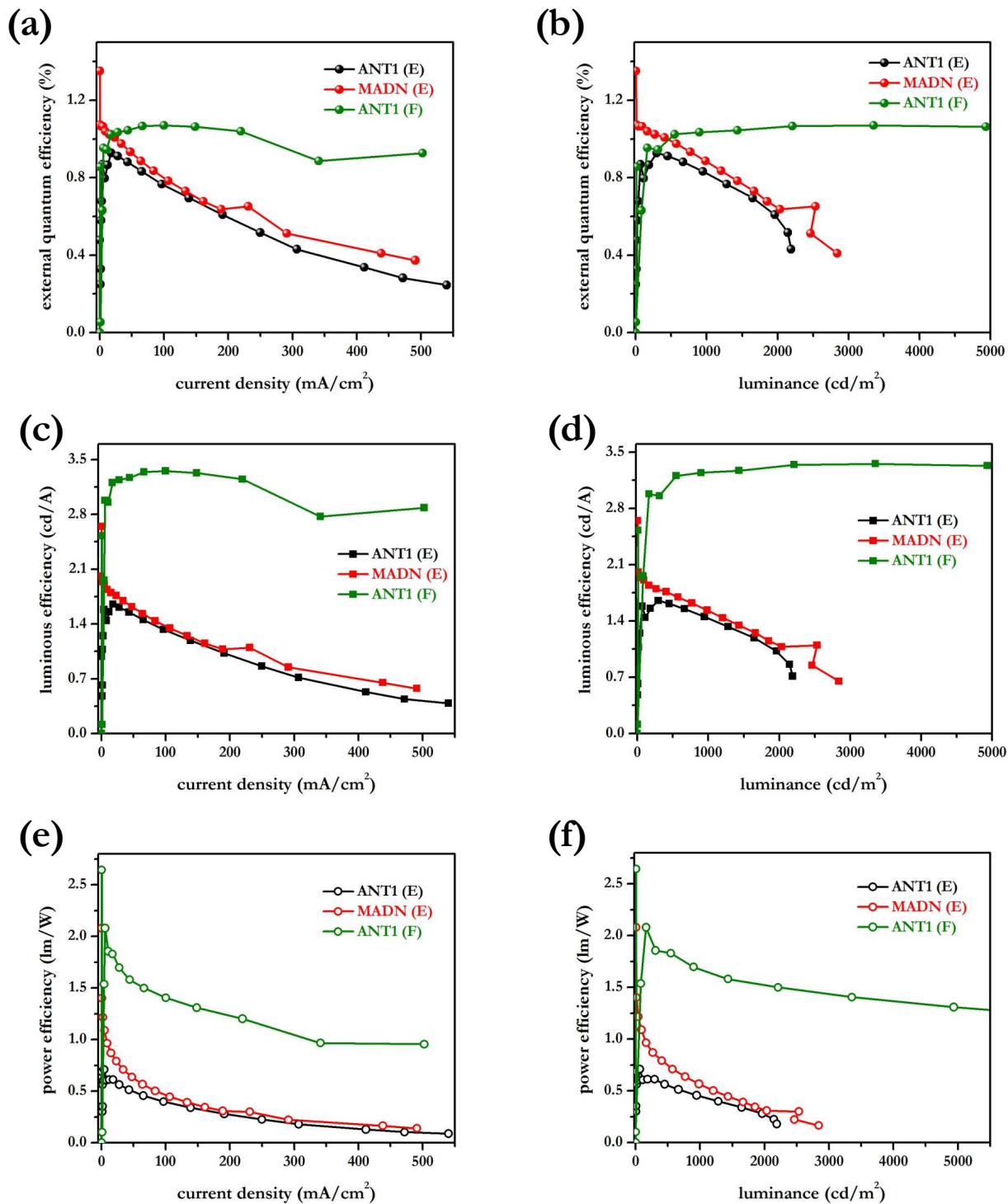


Fig. S7 Plots of external quantum efficiency vs current density (a), external quantum efficiency vs luminance (b), luminous efficiency vs current density (c), luminous efficiency vs luminance (d), power efficiency vs current density (e) and power efficiency vs luminance (f) for the devices of configurations E and F, refer to text.

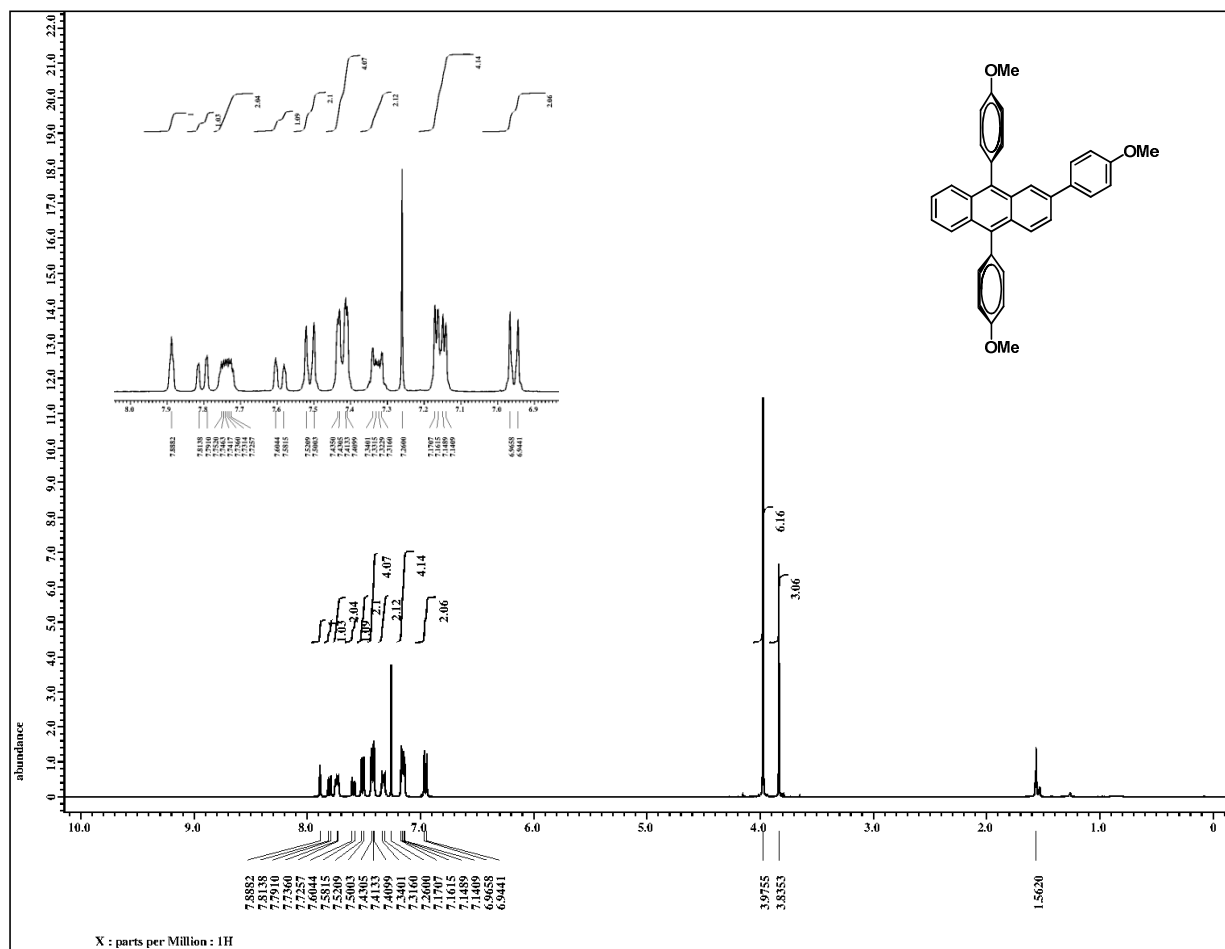


Fig. S8 ^1H (400 MHz, CDCl_3) NMR spectrum of ANT1.

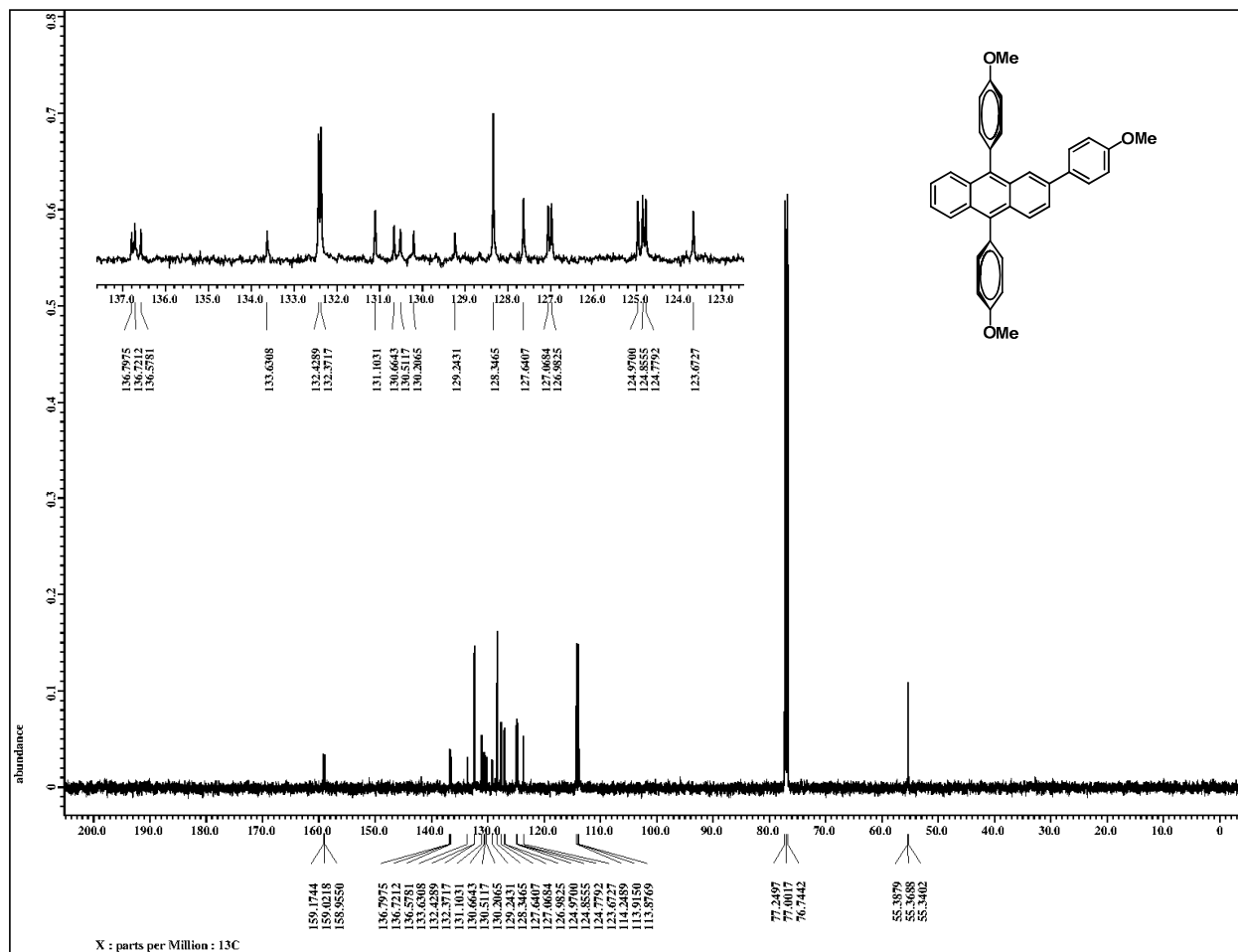


Fig. S9 ^{13}C NMR (CDCl_3 , 125 MHz) spectrum of ANT1.

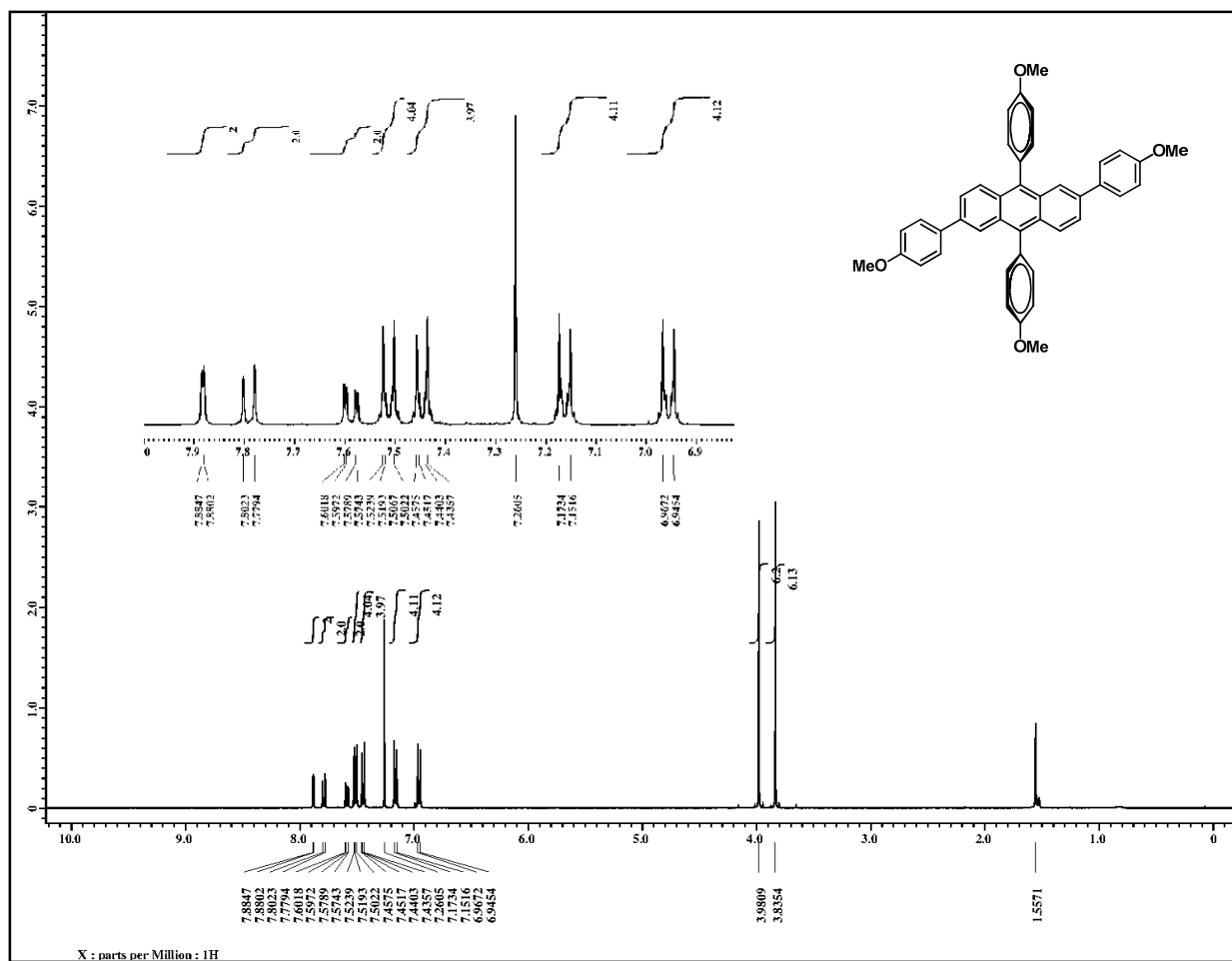


Fig. S10 ^1H (400 MHz, CDCl_3) NMR spectrum of ANT2.

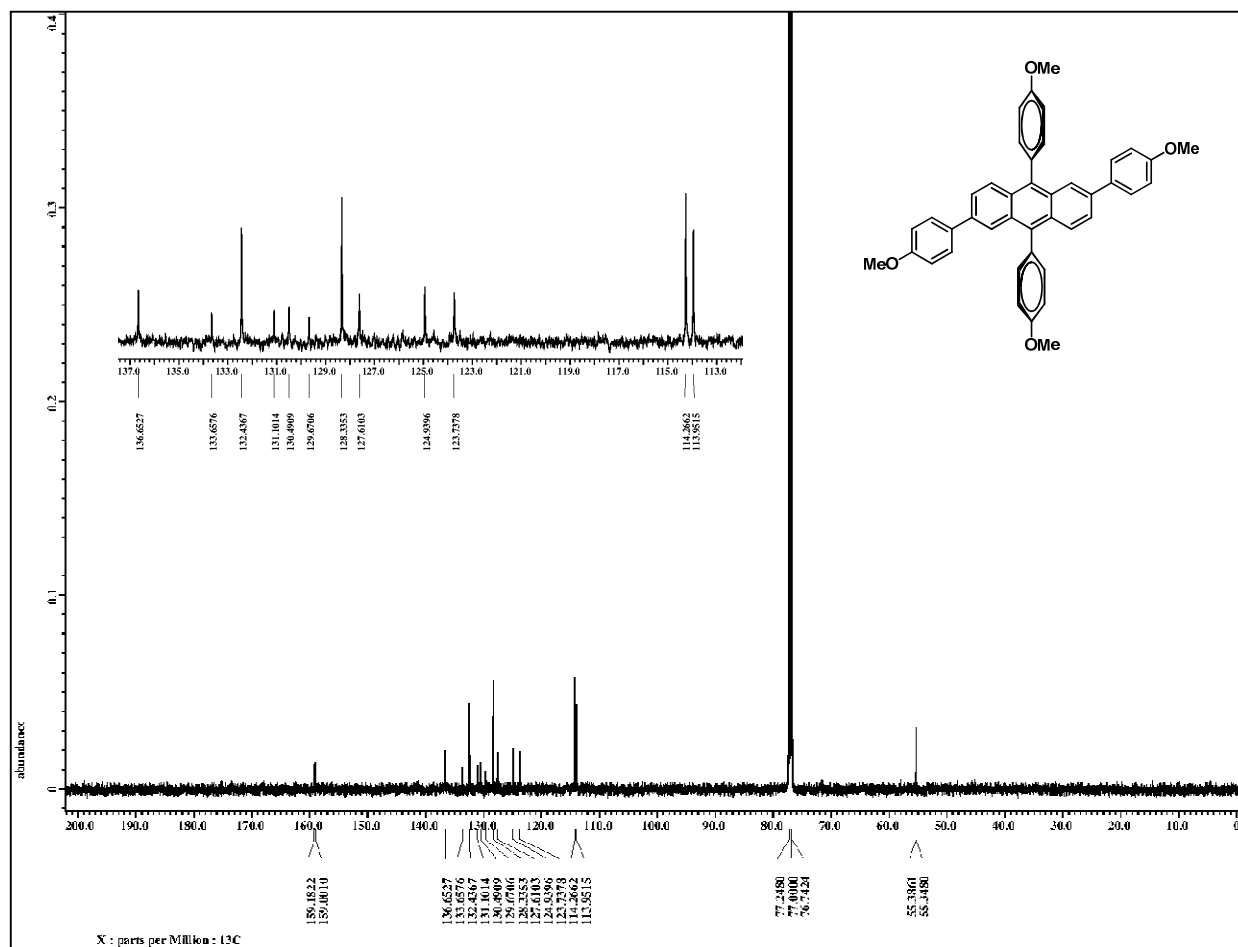


Fig. S11 ^{13}C NMR (125 MHz, CDCl_3) spectrum of ANT2.

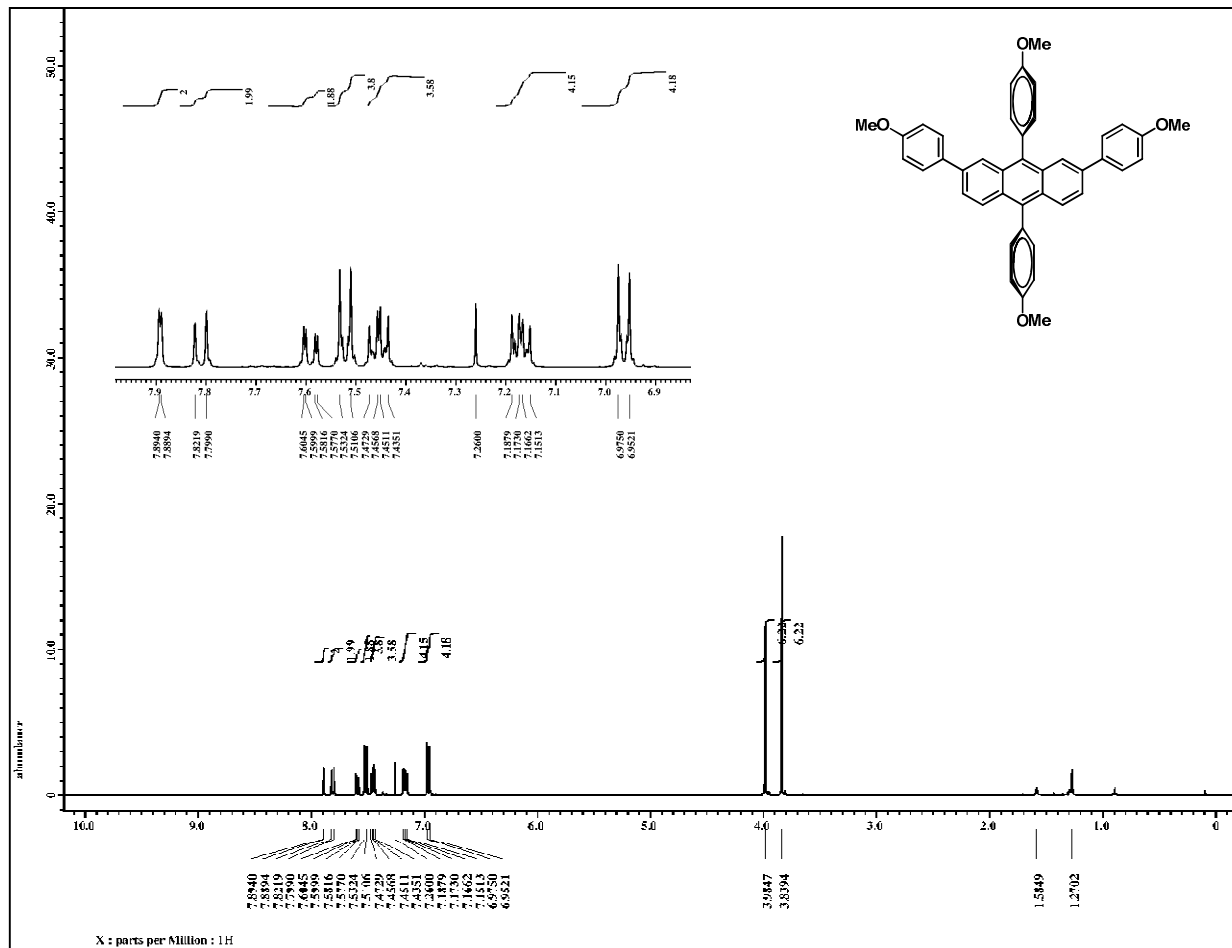


Fig. S12 ^1H (400 MHz, CDCl_3) NMR spectrum of ANT3.

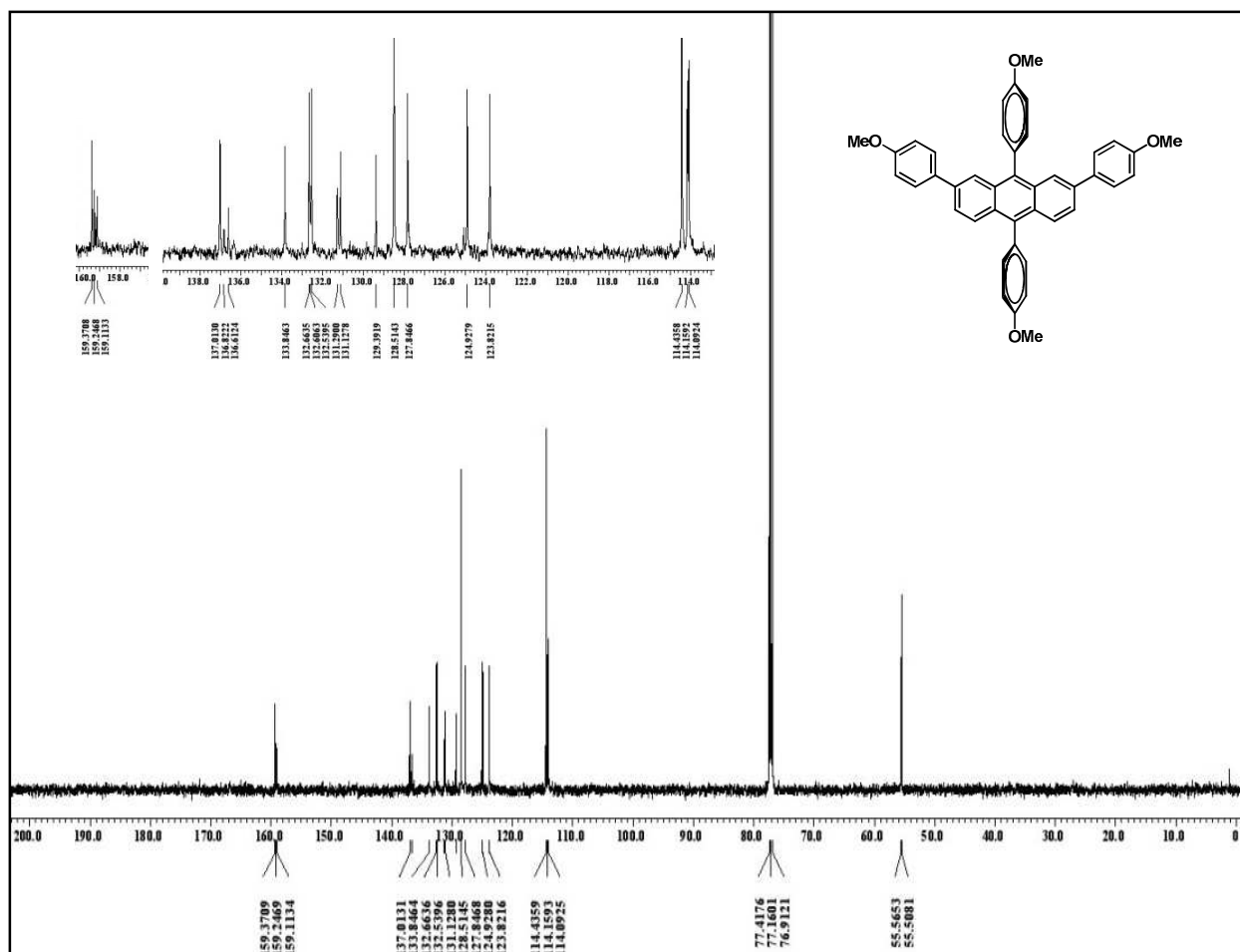


Fig. S13 ^{13}C NMR (125 MHz, CDCl_3) spectrum of ANT3.

X-ray crystal structure determinations. The crystals of suitable quality were mounted in glass capillaries, cooled to 0 and 100 K respectively, and the intensity data were collected on a Bruker Nonius SMART APEX CCD detector system with Mo-sealed Siemens ceramic diffraction tube ($\lambda = 0.71073$) and a highly oriented graphite monochromator operating at 50 kV and 30 mA. The data were collected on a hemisphere mode and processed with SAINT-Plus.^{S1} Empirical absorption corrections were made using SADABS.¹ The structures were solved by direct methods using SHELXTL package and refined by full matrix least-squares method based on F^2 using SHELX97 program.^{S2} All the nonhydrogen atoms were refined anisotropically. The hydrogen atoms were included in the ideal positions with fixed isotropic U values and were riding with their respective non-hydrogen atoms.

References

- S1 Bruker, SMART, SAINT-Plus, SADABS. Bruker Axs Inc. 1998 Madison, Wisconsin, USA.
- S2 G. M. Sheldrick, *Acta Cryst. A*, 2008, **64**, 112.

Table S1 Crystal data and structure refinements of **ANT2** and **ANT3**.

	ANT2	ANT3
	(CCDC No: 1507262)	(CCDC No: 1507231)
Formula	C ₄₂ H ₃₄ Cl ₃ O ₄ ·CHCl ₃	2(C ₄₂ H ₃₄ O ₄)·3CCl ₄
M	722.06	1666.81
T/K	100(2)	100(2)
Crystal size/mm ³	0.16 x 0.14 x 0.12	0.16 x 0.14 x 0.12
Crystal system	Monoclinic	Monoclinic
Space group	<i>P</i> 2 ₁	<i>P</i> 2 ₁
<i>a</i> /Å	12.8728(15)	15.7016(7)
<i>b</i> /Å	9.7876(11)	9.8725(5)
<i>c</i> /Å	15.2958(19)	25.8617(12)
<i>α</i> /(°)	90	90
<i>β</i> /(°)	112.529(4)	99.2320(10)
<i>γ</i> /(°)	90	90
<i>V</i> /Å ³	1780.1(4)	3957.0(3)
<i>Z</i> , <i>d</i> _{calcd} /(g cm ⁻³)	4, 1.291	2, 1.399
<i>μ</i> /mm ⁻¹	0.301	0.477
<i>F</i> (000)	752	1716
<i>θ</i> range/(°)	12.5–25.0	2.2–25.0
Index ranges	-15 ≤ <i>h</i> ≤ 13 -11 ≤ <i>k</i> ≤ 11 -18 ≤ <i>l</i> ≤ 18	-16 ≤ <i>h</i> ≤ 18 -11 ≤ <i>k</i> ≤ 11 -30 ≤ <i>l</i> ≤ 30
Reflections collected	14309	32037
Independent	6224	13877
Reflections	[<i>R</i> _{int} = 0.067]	[<i>R</i> _{int} = 0.0674]
Completeness	99.8%	99.9%
Data/restraints/parameters	6224/1/452	13877/1/1019
Goodness-of-fit on <i>F</i> ²	1.303	1.125
<i>R</i> ₁ , <i>wR</i> ₂ [<i>I</i> > 2σ(<i>I</i>)]	0.0962, 0.2254	0.0921, 0.2000
<i>R</i> ₁ , <i>wR</i> ₂ (all data)	0.1687, 0.2441	0.1725, 0.2233
Largest diff. peak, hole/(e Å ⁻³)	1.582, -0.659	1.147, -0.805

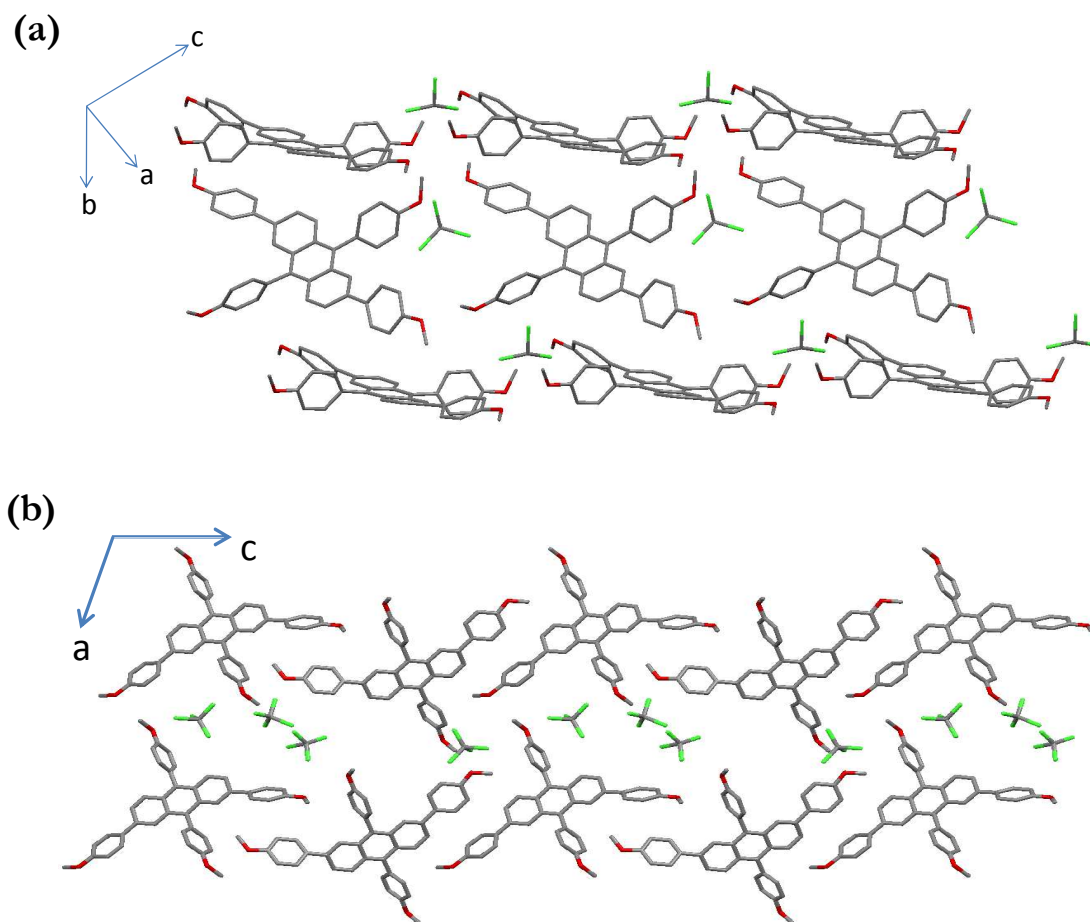


Fig. S14 (b) Crystal packing diagrams of ANT2 (a) and ANT3 (b). Notice the presence of chloroform and carbon tetrachloride molecules present as guests in the crystal lattices of ANT2 (a) and ANT3, respectively. For clarity, hydrogen atoms have been omitted.